Journal of Hazardous Materials 235–236 (2012) 47–53

Contents lists available at SciVerse ScienceDirect

Journal of Hazardous Materials

journal homepage: www.elsevier.com/locate/jhazmat

Pulmotoxicological effects caused by long-term titanium dioxide nanoparticles exposure in mice

Qingqing Sun[a,1], Danning Tan[a,1], Yuguan Ze[a,1], Xuezi Sang[a,1], Xiaorun Liu[b,c,1], Suxin Gui[a], Zhe Cheng[a], Jie Cheng[a], Renping Hu[a], Guodong Gao[a], Gan Liu[a], Min Zhu[a], Xiaoyang Zhao[a], Lei Sheng[a], Ling Wang[a], Meng Tang[b,c,**], Fashui Hong[a,*]

[a] Medical College of Soochow University, Suzhou 215123, China
[b] Key Laboratory of Environmental Medicine and Engineering, Ministry of Education, School of Public Health, Southeast University, Nanjing 210009, China
[c] Jiangsu Key Laboratory for Biomaterials and Devices, Southeast University, Nanjing 210009, China

HIGHLIGHTS

- Exposure to TiO_2 NPs could be significantly accumulated in the lung.
- Exposure to TiO_2 NPs caused pulmonary injury in mice.
- Exposure to TiO_2 NP promoted the expression of inflammatory cytokines in the lung.
- Exposure to TiO_2 NP caused ROS overproduction in the lung.

ARTICLE INFO

Article history:
Received 17 January 2012
Received in revised form 20 May 2012
Accepted 21 May 2012
Available online 27 May 2012

Keywords:
Titanium dioxide nanoparticles
Lung
Oxidative stress
Inflammation
Cytokines

ABSTRACT

Exposure to titanium dioxide nanoparticles (TiO_2 NPs) has been demonstrated to result in pulmonary inflammation in animals; however, very little is known about the molecular mechanisms of pulmonary injury due to TiO_2 NPs exposure. The aim of this study was to evaluate the oxidative stress and molecular mechanism associated with pulmonary inflammation in chronic lung toxicity caused by the intratracheal instillation of TiO_2 NPs for 90 consecutive days in mice. Our findings suggest that TiO_2 NPs are significantly accumulated in the lung, leading to an obvious increase in lung indices, inflammation and bleeding in the lung. Exposure to TiO_2 NPs significantly increased the accumulation of reactive oxygen species and the level of lipid peroxidation, and decreased antioxidant capacity in the lung. Furthermore, TiO_2 NPs exposure activated nuclear factor-κB, increased the levels of tumor necrosis factor-α, cyclooxygenase-2, heme oxygenase-1, interleukin-2, interleukin-4, interleukin-6, interleukin-8, interleukin-10, interleukin-18, interleukin-1β, and CYP1A1 expression. However, TiO_2 NPs exposure decreased NF-κB-inhibiting factor and heat shock protein 70 expression. Our results suggest that the generation of pulmonary inflammation caused by TiO_2 NPs in mice is closely related to oxidative stress and the expression of inflammatory cytokines.

1. Introduction

Titanium dioxide nanoparticles (TiO_2 NPs) are a white pigment widely used in paints, plastics, ceramics, rubber and cosmetics. The primary building blocks of TiO_2 NPs may become suspended in air during production, distribution, and use. Therefore, manufactured TiO_2 NPs can become a component of indoor and outdoor environments and thus may be present in the air we breathe. Because these particles are in the respirable size range, it is important to investigate the potential lung effects of TiO_2 NPs suspended in air as aerosols [1–3].

Over the past decade, various studies have unequivocally shown that TiO_2 NPs are able to enter into the interstitial spaces of the lung [4–6]. Importantly, previous studies demonstrated that exposure to TiO_2 NPs resulted in reactive oxygen species (ROS) accumulation in human or rat alveolar macrophages in vitro [7], elevated levels of lipid peroxidation, hydrogen peroxide radicals, alveolar macrophage numbers, and increased activities of glutathione peroxidase, glutathione reductase 6-phosphate glucose dehydrogenase, and glutathione S-transferase in rats, which showed that

* Corresponding author at: Medical College of Soochow University, Suzhou 215123, China. Tel.: +86 0512 61117563; fax: +86 0512 65880103.
** Corresponding author at: Key Laboratory of Environmental Medicine and Engineering, Ministry of Education, School of Public Health, Southeast University, Nanjing 210009, China.
E-mail addresses: tm@seu.edu.cn (M. Tang), Hongfsh_cn@sina.com (F. Hong).
[1] Contributed equally to this work.

0304-3894/$ – see front matter © 2012 Elsevier B.V. All rights reserved.
http://dx.doi.org/10.1016/j.jhazmat.2012.05.072

TiO_2 NPs induced the generation of antioxidant enzymes by a cellular self-protection mechanism without decreasing the free radical poisoning effect [8]. By exposing human bronchial epithelial cells to TiO_2 NPs, Gurr et al. also found that TiO_2 NPs induced DNA damage, lipid peroxidation, and micronuclei formation in vitro [9]. Grassian et al. demonstrated that exposing mice to TiO_2 NPs was essentially negative and showed reversible inflammation characterized by an increase in alveolar macrophages in lungs [10]. Furthermore, Hamilton Jr. et al. also suggested that TiO_2 NPs exposure can initiate an inflammatory reaction and induce inflammasome activation and the release of inflammatory cytokines through a cathepsin B-mediated mechanism in mouse lung [11]. Although these studies confirmed that TiO_2 NPs could enter the lung, resulting in oxidative stress and inflammatory responses, the molecular mechanism of TiO_2 NPs-induced pulmonary inflammation is unclear.

Therefore, in this study, mice were continuously exposed to 2.5, 5, or 10 mg/kg body weight TiO_2 NPs administered by intratracheal instillation for 90 consecutive days, and oxidative stress, alterations in the expression of inflammatory cytokines, and apoptosis in mouse lung were investigated to determine the mechanism of pulmonary inflammation caused by TiO_2 NPs exposure in mice.

2. Materials and methods

2.1. Chemicals and preparation

Nanoparticulate anatase TiO_2 was prepared via controlled hydrolysis of titanium tetrabutoxide. The details of the synthesis and characterization of TiO_2 NPs were previously described by Yang et al. [12] and Hu et al. [13], respectively. The average particle size contained in the powder suspended in 0.5% (w/v) hydroxypropylmethylcellulose (HPMC) K4 M solvent after 12 h and 24 h incubation ranged from 5 to 6 nm. The mean hydrodynamic diameter of the TiO_2 NPs in HPMC solvent ranged from 208 to 330 nm (mainly 294 nm), and the zeta potential after 12 h and 24 h incubation was 7.57 mV and 9.28 mV, respectively [13].

2.2. Animals and treatment

It was previously demonstrated by Wang et al. that sensitivity to TiO_2 exposure was higher in CD-1 (ICR) female mice than in CD-1 (ICR) male mice [5]. Therefore, CD-1 (ICR) female mice were used in this study. 80 CD-1 (ICR) female mice (24 ± 2 g) were purchased from the Animal Center of Soochow University (China). The mice were housed in stainless steel cages in a ventilated animal room. Room temperature of the housing facility was maintained at $24 \pm 2\,^{\circ}C$ with a relative humidity of $60 \pm 10\%$ and a 12-h light/dark cycle. Distilled water and sterilized food were available ad libitum. Prior to dosing, the mice were acclimated to this environment for 5 days. All animals were handled in accordance with the guidelines and protocols approved by the Care and Use of Animals Committee of Soochow University (China). All procedures used in the animal experiments conformed to the U.S. National Institutes of Health Guide for the Care and Use of Laboratory Animals [14].

For the experiment, the mice were randomly divided into four groups ($N = 20$), including a control group (treated with 0.5%, w/v, HPMC) and three experimental groups (2.5, 5, and 10 mg/kg BW TiO_2 NPs). The mice were weighed, and the TiO_2 NP suspensions were administered to the mice by intratracheal instillation every day for 90 days. Any symptoms or mortality were observed and recorded carefully every day during the 90-day period. After 90 days, the mice were first weighed, and then sacrificed after being anesthetized using ether.

2.3. Coefficient of lung

After weighing the body and lungs, the coefficient of lung to body weight was calculated as the ratio of lung (wet weight, mg) to body weight (g).

2.4. Titanium content analysis

Lungs were removed from storage at $-80\,^{\circ}C$ and then thawed. Approximately 0.2 g of the lung was weighed, digested and analyzed for titanium content. Inductively coupled plasma-mass spectrometry (ICP-MS, Thermo Elemental X7, Thermo Electron Co., USA) was used to analyze the titanium concentration in the samples. For the analysis, an Indium concentration of 20 ng/mL was utilized as an internal standard element, and the detection limit of titanium was 0.074 ng/mL. The data were expressed as nanograms per gram fresh tissue.

2.5. Histopathological examination of lung

For the pathological studies, all histopathological tests were performed using standard laboratory procedures [15]. The lungs were embedded in paraffin blocks, then sliced into sections 5 μm thick and placed onto glass slides. After hematoxylin–eosin (HE) staining, the slides were observed and photographs were taken using an optical microscope (Nikon U-III Multi-point Sensor System, USA). The pathologist was blind to the identity and analysis of the pathology slides.

2.6. Assay of cytokine expression

The levels of mRNA expression of nuclear factor-κB (NF-κB), NF-κB-inhibiting factor (IκB), tumor necrosis factor-α (TNF-α), interleukin-2 (IL-2), interleukin-4 (IL-4), interleukin-6 (IL-6), interleukin-8 (IL-8), interleukin-10 (IL-10), interleukin-18 (IL-18), interleukin-1β (IL-1β), cyclooxygenase 2 (COX-2), heme oxygenase-1 (HO-1), cytochrome p450 1A (CYP1A) and heat shock protein 70 (HSP70) in mouse lung were determined using real-time quantitative RT polymerase chain reaction (RT-PCR) [16–18]. Synthesized cDNA was used for real-time-PCR by employing primers that were designed using Primer Express Software according to the software guidelines. PCR primer sequences are available upon request. To determine NF-κB, IκB, TNF-α, IL-2, IL-4, IL-6, IL-8, IL-10, IL-18, IL-6, IL-1β, COX-2, HO-1, CYP1A1 and HSP-70 levels in mouse lung, ELISA was performed using commercial kits selective for each respective protein (R&D Systems, USA) following the manufacturer's instructions. The absorbance was measured on a microplate reader at 450 nm (Varioskan Flash, Thermo Electron, Finland), and the concentrations of NF-κB, IκB, TNF-α, IL-2, IL-4, IL-6, IL-8, IL-10, IL-18, IL-6, IL-1β, COX-2, HO-1, CYP1A1 and HSP-70 were calculated from a standard curve for each sample.

2.7. Assay of ROS and lipid peroxidation levels in lung

ROS assay: $O_2 \cdot^-$ in lung tissues was measured by monitoring the reduction of 3′-{1-[(phenylamino)carbonyl]-3,4-tetrazolium}–bis (4-methoxy-6-nitro) benzenesulfonic acid hydrate (XTT) in the presence of $O_2 \cdot^-$, as described by Oliveira et al. [19]. Detection of H_2O_2 in lung tissues was carried out using the xylenol orange assay [20].

Lipid peroxidation level in lung tissue was determined as the concentration of malondialdehyde (MDA) generated by the thiobarbituric acid reaction, as previously described by Buege and Aust [21].

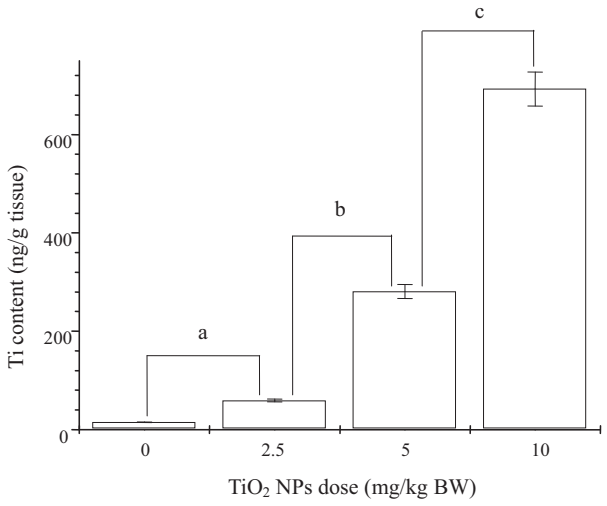

Fig. 1. The contents of titanium in the mouse lung after an intratracheal instillation with TiO_2 NPs for 90 consecutive days. Treatments with different letters indicate significantly different values ($p < 0.01$). Values represent means ± SE ($N = 5$).

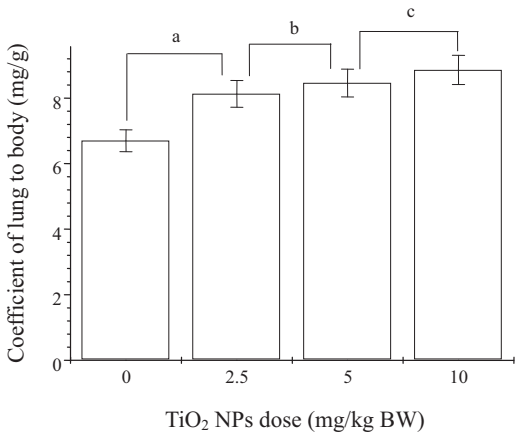

Fig. 2. The coefficients of lung of mice by an intratracheal instillation with TiO_2 NPs for 90 consecutive days. Treatments with different letters indicate significantly different values ($p < 0.05$). Values represent means ± SE ($N = 20$).

2.8. Assay of glutathione in lung

In order to perform the reduced glutathione (GSH) assay, the lungs were homogenized as described above. However, supernatants were not diluted five-fold as described in the case of the antioxidant enzyme assays. GSH contents were estimated using the method of Hissin and Hilf [22].

2.9. Statistical analysis

Statistical analyses were conducted using SPSS 17 software. Data were expressed as means ± standard error (SE). One-way analysis of variance (ANOVA) was carried out to compare the differences in means among multi-group data. Dunnett's test was performed when each dataset was compared with the solvent-control data. Statistical significance for all tests was judged at a probability level of 0.05 ($p < 0.05$).

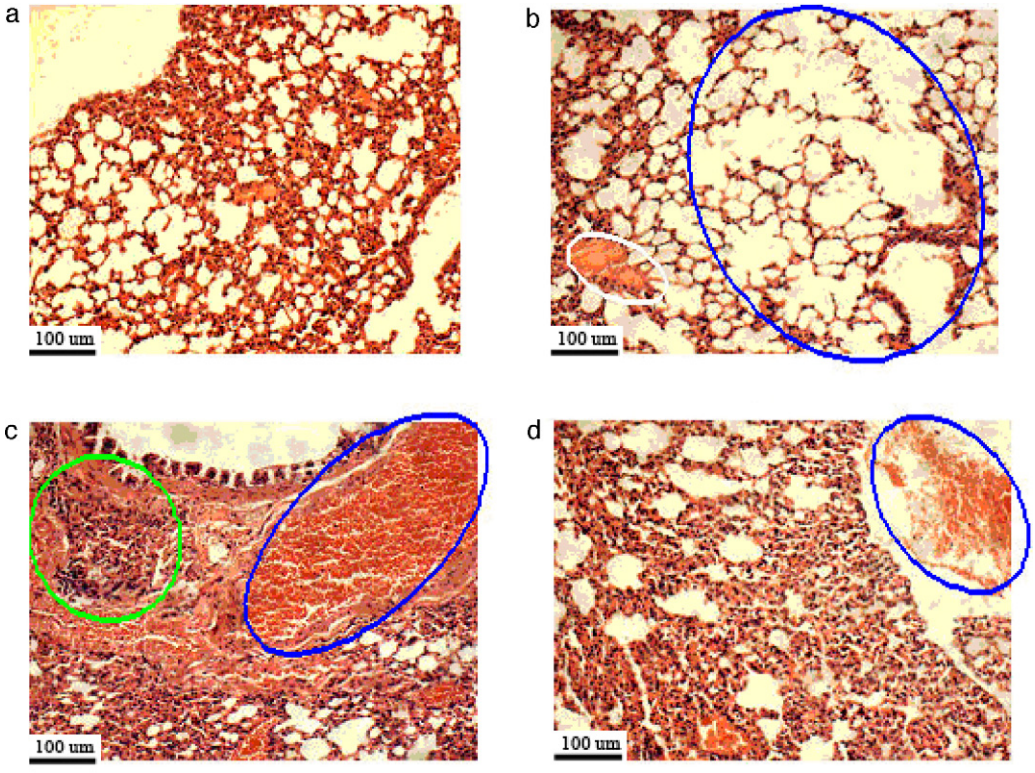

Fig. 3. Histopathological observation caused by an intratracheal instillation with TiO_2 NPs for 90 consecutive days. (a) Control group (unexposed mice) presents normal pulmonary alveoli; (b) 2.5 mg/kg TiO_2 NPs group presents pulmonary emphysema (blue cycle) and edema (white cycle); (c) 5 mg/kg TiO_2 NPs group indicates inflammatory cell infiltration (green cycle), congestion of blood vessel (blue arrow); (d) 10 mg/kg TiO_2 NPs group indicates pulmonary bleeding (blue cycle). (For interpretation of the references to color in the artwork, the reader is referred to the web version of the article.)

3. Results

3.1. Titanium accumulation and lung coefficient

Titanium accumulation in the lung was observed with increasing TiO_2 NPs dose (Fig. 1) ($p < 0.01$). Furthermore, exposure to TiO_2 NPs for 90 consecutive days caused significant increases in the coefficients of lung ($p < 0.05$ or $p < 0.01$) (Fig. 2). These results showed that accumulation of titanium in the lung was associated with the coefficients of lung in mice. The increase in lung indices caused by TiO_2 NPs exposure may be related to lung function impairment and lung injury, which were confirmed by histopathological observation of mouse lung and assays of biochemical parameters.

3.2. Lung histopathology

Fig. 3 shows the histopathological changes in lungs exposed to TiO_2 NPs. In mice treated with 2.5 mg/kg BW TiO_2 NPs, pulmonary tissue showed significant emphysema and edema. In mice treated with 5 mg/kg BW TiO_2 NPs, inflammatory cell infiltration, and congestion of blood vessels were observed (Fig. 3c). Furthermore, pulmonary bleeding was observed in mice treated with 10 mg/kg BW TiO_2 NPs (Fig. 3d). These findings indicated that lung injury due to TiO_2 NPs exposure occurred in a dose-dependent manner.

3.3. Cytokine expression

Histopathological observations indicated that injury and the inflammatory response occurred in mouse lung following exposure to TiO_2 NPs. To confirm the role of molecular mechanisms in TiO_2 NPs-induced lung injury, changes in the expression of inflammation-related genes or antioxidative capacity-related genes and their proteins caused by TiO_2 NP exposure in mice were assessed using real time RT-PCR and ELISA (Tables 1 and 2). It can be seen in Tables 1 and 2 that TiO_2 NP exposure resulted in significant increases in NF-κB, COX-2, HO-1, TNF-α, IL-2, IL-4, IL-6, IL-8, IL-10, IL-18, IL-1β, and CYP1A1 expression, while significant decreases in IκB and HSP-70 expression in mouse kidney compared with the control ($p < 0.05$ or 0.01) were observed, which were consistent with the trends in lung injury.

3.4. ROS accumulation and lipid peroxidation level

To further confirm molecular mechanisms in TiO_2 NPs-induced lung injury, we determined the rate of ROS generation and MDA content in lung. The effects of TiO_2 NPs on the rate of $O_2\cdot^-$ and H_2O_2 generation and MDA content in mouse lungs are shown in Figs. 4 and 5. The rate of $O_2\cdot^-$ and H_2O_2 generation and MDA content in the lung in the 2.5, 5, and 10 mg TiO_2 NPs-treated groups were significantly different from the control ($p < 0.05$ or 0.01), indicating that exposure to long-term low dose TiO_2 NPs resulted in oxidative stress in the lung.

3.5. GSH content of lung

GSH content in the mouse lung following exposure to TiO_2 NPs is presented in Fig. 6. With increasing doses of TiO_2 NPs, the GSH content in the lung was significantly decreased ($p < 0.05$ or 0.01), suggesting that TiO_2 NPs exposure decreased the antioxidant capacity of the lung.

4. Discussion

The present study suggests that the intratracheal instillation of TiO_2 NPs at doses of 2.5, 5, and 10 mg/kg BW for 90 consecutive days

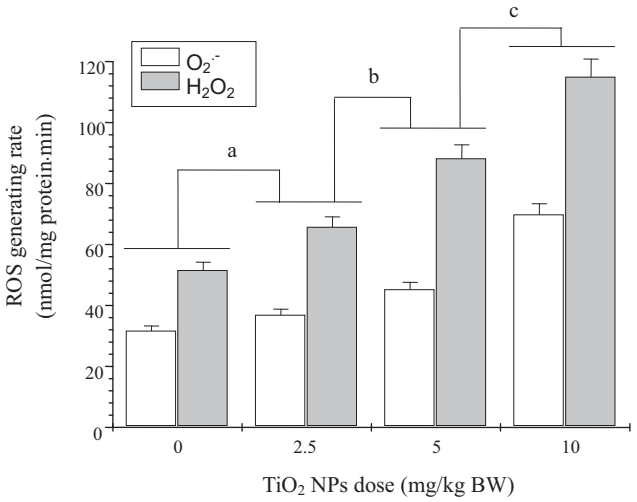

Fig. 4. ROS accumulation of the mouse lung after an intratracheal instillation with TiO_2 NPs for 90 consecutive days. Treatments with different letters indicate significantly different values ($p < 0.05$). Values represent means ± SE ($N = 5$).

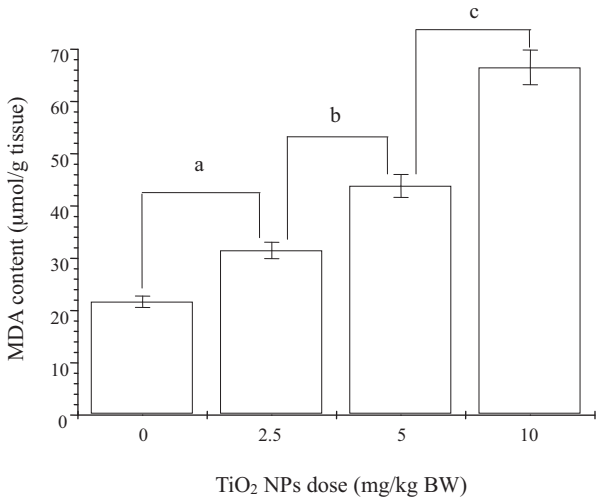

Fig. 5. MDA contents of the mouse lung after an intratracheal instillation with TiO_2 NPs for 90 consecutive days. Treatments with different letters indicate significantly different values ($p < 0.05$). Values represent means ± SE ($N = 5$).

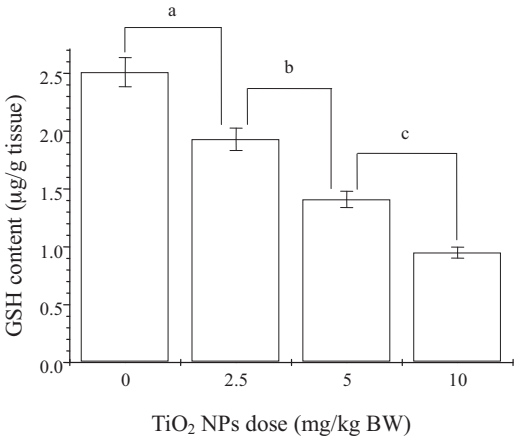

Fig. 6. The GSH content of the mouse lung after an intratracheal instillation with TiO_2 NPs for 90 consecutive days. Treatments with different letters indicate significantly different values ($p < 0.05$). Values represent means ± SE ($N = 5$).

Table 1
Effect of TiO_2 NPs on the amplification of regulating the inflammation, immune and oxidative stress gene mRNA of the mouse lung by real-time PCR analysis after an intratracheal instillation with TiO_2 NPs for 90 consecutive days.

Ratio of gene/actin	TiO_2 NPs (mg/kg BW)			
	0	2.5	5	10
NF-κB/actin	0.39 ± 0.020a	0.47 ± 0.023b	0.73 ± 0.037c	1.23 ± 0.062d
IκB/actin	0.66 ± 0.033a	0.51 ± 0.026b	0.39 ± 0.020c	0.26 ± 0.013d
COX-2/actin	0.59 ± 0.030a	0.72 ± 0.036b	0.96 ± 0.048c	1.23 ± 0.062d
HO-1/actin	0.85 ± 0.043a	1.14 ± 0.057b	2.06 ± 0.103c	3.174 ± 0.159d
TNF-α/actin	0.08 ± 0.004a	0.11 ± 0.006b	0.19 ± 0.010c	0.28 ± 0.014d
IL-2/actin	0.05 ± 0.003a	0.08 ± 0.004b	0.12 ± 0.006c	0.18 ± 0.009d
IL-4/actin	0.05 ± 0.003a	0.07 ± 0.004b	0.11 ± 0.006c	0.16 ± 0.008d
IL-6/actin	0.04 ± 0.002a	0.06 ± 0.003b	0.09 ± 0.005c	0.13 ± 0.007d
IL-8/actin	0.05 ± 0.003a	0.08 ± 0.004b	0.10 ± 0.005c	0.14 ± 0.007d
IL-10/actin	0.08 ± 0.004a	0.11 ± 0.006b	0.14 ± 0.007c	0.18 ± 0.009d
IL-18/actin	0.28 ± 0.014a	0.34 ± 0.017b	0.41 ± 0.021c	0.52 ± 0.026d
IL-1β/actin	0.16 ± 0.008a	0.21 ± 0.011b	0.31 ± 0.016c	0.39 ± 0.020d
CYP1A1/actin	0.37 ± 0.019a	0.46 ± 0.023b	0.73 ± 0.037c	1.05 ± 0.053d
HSP-70/actin	0.31 ± 0.016a	0.26 ± 0.013b	0.21 ± 0.011c	0.12 ± 0.006d

Treatments with different letters indicate significantly different values ($p < 0.05$). Values represent means ± SE ($N = 5$).

can be accumulated in mouse lung (Fig. 1). Furthermore, the accumulated TiO_2 NPs can significantly increase lung indices (Fig. 2), and induce histopathological changes in the lung, such as emphysema, edema, inflammatory cell infiltration, congestion of blood vessels and pulmonary bleeding (Fig. 3). Warheit et al. demonstrated that exposure to intratracheal instillation of TiO_2 NPs produced pulmonary inflammatory responses in the rat lung [23,24]. Adult male ICR mice exposed to a single intratracheal dose of 0.1 or 0.5 mg TiO_2 NPs, showed emphysema, macrophage accumulation, extensive disruption of alveolar septa, type II pneumocyte hyperplasia, and epithelial cell apoptosis in the lung [25]. Chen et al. observed alveolar septal thickening, neutrophil infiltration, and thrombosis in the pulmonary vascular system in mice after an intraperitoneal injection of 324, 648, 972, 1296, 1944 and 2592 mg/kg BW TiO_2 NPs (3.6 nm) for 7 days, respectively, which demonstrated the generation of inflammation and the blockage of blood vessels in mouse lung [26]. However, Wang et al. suggested that a fixed large dose of 5 g/kg BW of TiO_2 NPs for 14 days did not result in abnormal changes in mouse lung [5]. The present study suggests that chronic lung injury in mice may be triggered by oxidative stress and alterations in the expression of inflammatory cytokines caused by TiO_2 NPs which resulted in the generation of inflammation and bleeding in the lung.

The current study was undertaken to address the mechanisms of NF-κB activation in pulmonary inflammation caused by TiO_2 NPs in mice. In our previous studies, we showed that TiO_2 NPs exposure led to increased NF-κB expression in the liver, spleen, and kidney of mice [27–31]. In the present study, we have provided further in vivo evidence for the activation of the classical NF-κB pathway in mouse lung, which involves a reduction in IκB expression (Tables 1 and 2). COX-2 is a classic pro-inflammatory gene induced by NF-κB, and is known to occupy an important position in the regulation of pulmonary inflammation [32]. In the present study, COX-2 expression was significantly induced in vivo following TiO_2 NPs exposure (Tables 1 and 2). In addition, we observed a significant increase in HO-1 expression in the TiO_2 NPs-exposed mouse lung (Tables 1 and 2). HO-1 induction is considered a sensitive oxidative stress marker [33] and has been shown to be increased in spleen tissue of TiO_2 NPs-exposed mice [30]. These findings provided further support for the well-known role of oxidative stress in TiO_2 NPs-elicited pathology [13,30,34,35]. The evaluation of NF-κB pathway activation on multiple levels is necessary, as there may be different mechanisms involved. While cytokines such as TNF-α, IL-1β, IL-2, IL-4, IL-6, IL-8, IL-10, and IL-18 induce the canonical pathway characterized by IκB degradation, exposure to TiO_2 NPs has also been shown to activate NF-κB in the liver via reduction of IκB expression [29]. These inflammatory cytokines are considered important factors in the development of silicosis [12–14] and are well-known inducers of NF-κB in various cell types [8–11]. Our data demonstrate that TiO_2 NPs exposure can significantly induce TNF-α, IL-1β, IL-2, IL-4, IL-6, IL-8, IL-10, and IL-18 expression (Tables 1 and 2), suggesting that these cytokines play crucial roles in TiO_2 NPs-induced NF-κB activation in the lung. This is in accordance with previous investigations in our laboratory [27].

Table 2
Effect of TiO_2 NPs on the inflammatory cytokin protein levels of the mouse lung by ELISA analysis after an intratracheal instillation with TiO_2 NPs for 90 consecutive days.

Protein expression	TiO_2 NPs (mg/kg BW)			
	0	2.5	5	10
NF-κB(ng/g tissue)	50.20 ± 2.51a	60.81 ± 3.04b	75.65 ± 3.78c	96.41 ± 4.82d
IκB(ng/g tissue)	13.69 ± 0.68a	10.51 ± 0.53b	8.98 ± 0.45c	7.64 ± 0.38d
COX-2(ng/g tissue)	30.53 ± 1.53a	48.43 ± 2.42b	61.37 ± 3.07c	75.87 ± 3.79d
HO-1(pg g tissue)	22.16 ± 1.11a	31.73 ± 1.59b	45.72 ± 2.29c	65.19 ± 3.26d
TNF-α(ng/g tissue)	19.05 ± 0.95a	33.33 ± 1.67b	47.75 ± 2.39c	68.09 ± 3.40d
IL-2(ng/g tissue)	16.17 ± 0.81a	26.43 ± 1.32b	37.77 ± 1.89c	48.89 ± 2.44d
IL-4(ng/g tissue)	33.80 ± 1.69a	48.35 ± 2.42b	66.06 ± 3.30c	87.84 ± 4.39d
IL-6(ng/g tissue)	10.78 ± 0.54a	18.81 ± 0.94b	30.97 ± 1.55c	41.22 ± 2.06d
IL-8(ng/g tissue)	53.66 ± 2.68a	73.73 ± 3.69b	86.62 ± 4.33c	105.68 ± 5.28d
IL-10(ng/g tissue)	20.65 ± 1.03a	30.70 ± 1.54b	42.85 ± 2.14c	59.99 ± 3.00d
IL-18(ng/g tissue)	61.66 ± 3.08a	82.83 ± 4.14b	105.98 ± 5.30c	131.59 ± 6.58d
IL-1β(ng/g tissue)	153.20 ± 7.66a	203.48 ± 10.17b	254.66 ± 12.73c	315.87 ± 15.79d
CYP1A1(ng/g tissue)	8.06 ± 0.40a	12.36 ± 0.62b	17.85 ± 0.89c	22.81 ± 1.14d
HSP-70(ng/g tissue)	30.49 ± 1.52a	23.82 ± 1.19b	17.09 ± 0.85c	11.14 ± 0.56d

Treatments with different letters indicate significantly different values ($p < 0.05$). Values represent means ± SE ($N = 5$).

To address the potential role of ROS in NF-κB activation in the lung, the accumulation of $O_2\cdot^-$ and H_2O_2 in lung was evaluated, which showed that TiO_2 NPs exposure significantly increased ROS and lipid peroxidation levels (Figs. 4 and 5). H_2O_2 is known to possess NF-κB activating properties, albeit in a cell specific-manner [36,37]. H_2O_2 is formed upon the dismutation of superoxide anions which are generated in large amounts by activated macrophages during inflammation. The generation of ROS in mouse lung was not only shown in this study to be TiO_2 NPs-concentration dependent, but also led to a notable reduction in IκB expression in the lung. This finding may be due to the fact that H_2O_2 has been found to activate NF-κB through a classical pathway in the lung, involving IκB expression. In line with these observations, we also observed an obvious decrease in GSH content in the lung caused by TiO_2 NPs exposure (Fig. 6). In alveolar epithelial cells, GSH is considered to be the most important intracellular antioxidant [38]. Lower levels of intracellular GSH have been associated with enhanced NF-κB activation [39]. In Jurkat cells, increased intracellular GSH levels have been shown to block H_2O_2-induced NF-kB activation [36]. There is also evidence for the interplay between ROS and cytokines in NF-κB induction [40]. Our findings suggest that oxidative stress is a key mechanism in the activation of NF-κB in mouse lung caused by TiO_2 NPs exposure. This is evidenced by the ability of H_2O_2 to activate NF-κB, as well as the finding that modulation of the intracellular antioxidant level influenced classical NF-κB pathway activation.

In addition, our data suggest that TiO_2 NPs exposure significantly increased CYP1A expression, but caused a significant reduction in HSP70 expression in the lung (Tables 1 and 2). CYP1A and HSP70 represent different processes that cells follow to detoxify and/or defend against environmental toxicants. Therefore, the increase in CYP1A expression and reduction in HSP70 expression in the lung after 90 days exposure to TiO_2 NPs imply a slow biotransformation/detoxification in the lung [41–43].

5. Conclusion

The current study showed that mice treated with 2.5, 5 and 10 mg/kg BW TiO_2 NPs for 90 consecutive days showed lung injury, which was associated with alterations in inflammatory-related cytokines and oxidative stress. Our findings also underscore the importance of further elucidation of the involvement of NF-κB-dependent signaling pathways in the development and progression of pulmonary disorders induced by TiO_2 NPs exposure.

Acknowledgements

This work was supported by the National Natural Science Foundation of China (grant nos. 30901218, 81172697), National Important Project on Scientific Research of China (grant no. 2011CB933404), A Project Funded by the Priority Academic Program Development of Jiangsu Higher Education Institutions, and the National New Ideas Foundation of Student of China (grant no. 111028534).

References

[1] J.J. Bang, L.E. Murr, Atmospheric nanoparticles: preliminary studies and potential respiratory health risks for emerging nanotechnologies, J. Mater. Sci. Lett. 21 (2002) 361–366.
[2] G. Oberdörster, E. Oberdörster, J. Oberdörster, Nanotoxicology: an emerging discipline evolving from studies of ultrafine particles, Environ. Health Persp. 113 (2005) 823–839.
[3] R. Wilson, J. Spengler, Emissions, dispersion and concentration of particles, in: R. Wilson, J. Spengler (Eds.), Particles in Our Air: Concentrations and Health Effects, Harvard University Press, Cambridge, MA, 1996, pp. 41–84.
[4] G. Oberdörster, J. Ferin, R. Gelein, S.C. Soderholm, J. Finkelstein, Role of the alveolar macrophage in lung injury: studies with ultrafine particles, Environ. Health Persp. 97 (1992) 193–199.
[5] J.X. Wang, G.Q. Zhou, C.Y. Chen, H.W. Yu, T.C. Wang, Y.M. Ma, G. Jia, Y.X. Gao, B. Li, J. Sun, Y.F. Li, F. Jia, Y.L. Zhao, Z.F. Chai, Acute toxicity and biodistribution of different sized titanium dioxide particles in mice after oral administration, Toxicol. Lett. 168 (2007) 176–185.
[6] H.T. Liu, L.L. Ma, J.F. Zhao, J. Liu, J.Y. Yan, J. Ruan, F.S. Hong, Biochemical toxicity of nano-anatase TiO_2 particles in mice, Biol. Trace Elem. Res. 129 (2009) 170–180.
[7] Q. Rahman, J. Norwood, G. Oberdörster, G. Hatch, Rat–human differences in macrophage oxidant production by pollutant particles, in: Colloquium on Particulate Air Pollution and Human Mortality and Morbidity, January, Irvine, CA, USA, 1994, pp. 24–25.
[8] F. Afaq, P. Abidi, R. Matin, Q. Rahman, Cytotoxicity pro-oxidant effects and antioxidant depletion in rat lung alveolar macrophages exposed to ultrafine titanium dioxide, J. Appl. Toxicol. 18 (1998) 307–312.
[9] J. Gurr, C. Ass Wang, K.J. Chen, Ultrafine titanium dioxide particle in the absence of photoactivation can induce oxidative damage to human bronchial epithelial cells, Toxicology 213 (2005) 66–73.
[10] V.H. Grassian, P.T. O'Shaughnessy, A. Adamcakova-Dodd, J.M. Pettibone, P.S. Thorne, Inhalation exposure study of titanium dioxide nanoparticles with a primary particle size of 2–5 nm, Environ. Health Persp. 115 (2007) 397–402.
[11] R.F. Hamilton Jr., N.Q. Wu, D. Porter, M. Buford, M. Wolfarth, A. Holian, Particle length-dependent titanium dioxide nanomaterials toxicity and bioactivity, Particle Fibre Toxicol. 6 (2009) 35–645.
[12] P. Yang, C. Lu, N. Hua, Y. Du, Titanium dioxide nanoparticles co-doped with Fe^{3+} and Eu^{3+} ions for photocatalysis, Mater. Lett. 57 (2002) 794–801.
[13] R.P. Hu, L. Zheng, T. Zhang, Y.L. Cui, G.D. Gao, Z. Cheng, J. Chen, M. Tang, F.S. Hong, Molecular mechanism of hippocampal apoptosis of mice following exposure to titanium dioxide nanoparticles, J. Hazard. Mater. 191 (2011) 32–40.
[14] National Institutes of Health (NIH), Guide for the Care and Use of Laboratory Animals, National Academy Press, Washington, DC, 1996.
[15] A.B. Tarabishy, B. Aldabagh, Y. Sun, Y. Imamura, P.K. Mukherjee, J.H. Lass, M.A. Ghannoum, E. Pearlman, MyD88 regulation of Fusarium keratitis is dependent on TLR4 and IL-1R1 but not TLR2, J. Immunol. 181 (2008) 593–600.
[16] K.J. Livak, T.D. Schmittgen, Analysis of relative gene expression data using real-time quantitative PCR and the 2(−Delta Delta C(T)) method, Methods 25 (2001) 402–408.
[17] W.H. Liu, A. David, Saint validation of a quantitative method for real time PCR kinetics, Biochem. Biophys. Res. Commun. 294 (2002) 347–353.
[18] L.D. Ke, Z. Chen, A reliability test of standard-based quantitative PCR: exogenous vs endogenous standards, Mol. Cell Probes 14 (2) (2000) 127–135.
[19] C.P. Oliveira, F.P. Lopasso, F.R. Laurindo, R.M. Leitao, A.A. Laudanna, Protection against liver ischemia-reperfusion injury in rats by silymarin or verapamil, Transplant. Proc. 33 (2001) 3010–3014.
[20] J. Nourooz-Zadeh, J. Tajaddini-Sarmadi, S.P. Wolff, Measurement of plasma hydroperoxide concentrations by the ferrous oxidation-xylenol orange assay in conjunction with triphenylphosphine, Anal. Biochem. 220 (1994) 403–409.
[21] J.A. Buege, S.D. Aust, Microsomal lipid peroxidation, Methods Enzymol. 52 (1978) 302–310.
[22] P.J. Hissin, R. Hilf, A fluorometric method for determination of oxidized and reduced glutathione in tissues, Anal. Biochem. 74 (1976) 214–226.
[23] D.B. Warheit, T.R. Webb, C.M. Sayes, V.L. Colvin, K.L. Reed, Pulmonary instillation studies with nanoscale TiO_2 rods and dots in rats: toxicity is not dependent upon particle size and surface area, Toxicol. Sci. 91 (1) (2006) 227–236.
[24] D.B. Warheit, T.R. Webb, K.L. Reed, S. Frerichs, C.M. Sayes, Pulmonary toxicity study in rats with three forms of ultrafine-TiO_2 particles: differential responses related to surface properties, Toxicology 230 (2007) 90–104.
[25] H.W. Chen, S.F. Su, C.T. Chien, W.H. Lin, S.L. Yu, C.C. Chou, J.W. Chen, P.C. Yang, Titanium dioxide nanoparticles induce emphysema-like lung injury in mice, FASEB J. 20 (2006) 1732–1741.
[26] J.Y. Chen, X. Dong, J. Zhao, G.P. Tang, In vivo acute toxicity of titanium dioxide nanoparticles to mice after intraperitoneal injection, J. Appl. Toxicol. 29 (2009) 330–337.
[27] L.L. Ma, J.F. Zhao, J. Wang, Y.M. Duan, J. Liu, N. Li, H.T. Liu, J.Y. Yan, J. Ruan, F.S. Hong, The acute liver injury in mice caused by nano-anatase TiO_2, Nanoscale Res. Lett. 4 (2009) 128–275.
[28] Y.M. Duan, J. Liu, L.L. Ma, N. Li, H.T. Liu, J. Wang, L. Zheng, C. Liu, X.F. Wang, X.G. Zhang, J.Y. Yan, H. Wang, F.S. Hong, Toxicological characteristics of nanoparticulate anatase titanium dioxide in mice, Biomaterials 31 (2010) 894–899.
[29] Y.L. Cui, H.T. Liu, M. Zhou, Y.M. Duan, N. Li, X.L. Gong, R.P. Hu, M.M. Hong, F.S. Hong, Signaling pathway of inflammatory responses in the mouse liver caused by TiO_2 nanoparticules, J. Biomed. Mater. Res. Part A 96 (1) (2011) 221–229.
[30] J. Wang, N. Li, L. Zheng, Y. Wang, Y.M. Duan, S.S. Wang, X.Y. Zhao, Y.L. Cui, M. Zhou, J.W. Cai, S.J. Gong, H. Wang, F.S. Hong, P38-Nrf-2 signaling pathway of oxidative stress in mice caused by nanoparticulate TiO_2, Biol. Trace Elem. Res. 140 (2011) 186–197.
[31] S.X. Gui, Z.L. Zhang, L. Zheng, Y.L. Cui, X.R. Liu, N. Li, X.Z. Sang, Q.Q. Sun, G.D. Gao, Z. Cheng, J. Cheng, L. Wang, M. Tang, F.S. Hong, Molecular mechanism of kidney injury of mice caused by exposure to titanium dioxide nanoparticles, J. Hazard. Mater. 195 (2011) 365–370.
[32] G.Y. Park, J.W. Christman, Involvement of cyclooxygenase-2 and prostaglandins in the molecular pathogenesis of inflammatory lung diseases, Am. J. Physiol. Lung Cell Mol. Physiol. 290 (2006) L797–L805.
[33] N. Li, M. Wang, T.D. Oberley, J.M. Sempf, A.E. Nel, Comparison of the pro-oxidative and proinflammatory effects of organic diesel exhaust particle chemicals in bronchial epithelial cells and macrophages, J. Immunol. 169 (8) (2002) 4531–4541.

[34] L.L. Ma, J. Liu, N. Li, J. Wang, Y.M. Duan, J.Y. Yan, H.T. Liu, H. Wang, F.S. Hong, Oxidative stress in the brain of mice caused by translocated nanoparticulate TiO_2 delivered to the abdominal cavity, Biomaterials 31 (2010) 99–105.
[35] Y.L. Cui, X.L. Gong, Y.M. Duan, N. Li, R.P. Hu, H.T. Liu, M.M. Hong, M. Zhou, L. Wang, H. Wang, F.S. Hong, Hepatocyte apoptosis and its molecular mechanisms in mice caused by titanium dioxide nanoparticles, J. Hazard. Mater. 183 (2010) 874–880.
[36] R. Schreck, P. Rieber, P.A. Baeuerle, Reactive oxygen intermediates as apparently widely used messengers in the activation of the NF-kappa B transcription factor and HIV-1, EMBO J. 10 (8) (1991) 2247–2258.
[37] P. Brennan, L.A. O'Neill, Effects of oxidants and antioxidants on nuclear factor kappa B activation in three different cell lines: evidence against a universal hypothesis involving oxygen radicals, Biochim. Biophys. Acta 1260 (2) (1995) 167–175.
[38] I. Rahman, B. Mulier, P.S. Gilmour, T. Watchorn, K. Donaldson, P.K. Jeffery, W. MacNee, Oxidant-mediated lung epithelial cell tolerance: the role of intracellular glutathione and nuclear factor-kappaB, Biochem. Pharmacol. 62 (6) (2001) 787–794.
[39] S.P. Hehner, R. Breitkreutz, G. Shubinsky, H. Unsoeld, K. Schulze-Osthoff, M.L. Schmitz, W. Dröge, Enhancement of T cell receptor signaling by a mild oxidative shift in the intracellular thiol pool, J. Immunol. 165 (8) (2000) 4319–4328.
[40] Y.M. Janssen-Heininger, I. Macara, B.T. Mossman, Cooperativity between oxidants and tumor necrosis factor in the activation of nuclear factor (NF)-kappaB: requirement of Ras/mitogen-activated protein kinases in the activation of NF-kappaB by oxidants, Am. J. Respir. Cell Mol. Biol. 20 (5) (1999) 942–952.
[41] H.M. Beere, B.B. Wolf, K. Cain, D.D. Mosser, A. Mahboubi, T. Kuwana, P. Tailor, R.I. Morimoto, G.M. Cohen, D.R. Green, Heat-shock protein 70 inhibits apoptosis by preventing recruitment of procaspase-9 to the Apaf-1 apoptosome, Nat. Cell Biol. 2 (2000) 469–475.
[42] H.M. Li, T. Niki, T. Taira, S.M. Iguchi-Ariga, H. Ariga, Association of DJ-1 with chaperones and enhanced association and colocalization with mitochondrial Hsp70 by oxidative stress, Free Radic. Res. 39 (2005) 1091–1099.
[43] H.N. Hong, H.N. Kim, K.S. Park, S.K. Lee, M.B. Gu, Analysis of the effects diclofenac has on Japanese medaka (*Oryzias latipes*) using real-time PCR, Chemosphere 67 (2007) 2115–2121.